Proceedings of the Reactor Physics Asia 2023 (RPHA2023) Conference
Gyeongju, Korea, October 24-26, 2023

Radiation Field Analysis of a Heat Pipe Cooled Reactor for Underwater Application

Fanchen Li[a], Youqi Zheng[a*], Yushan Tao[a,b]
[a] *School of Nuclear Science and Technology, Xi'an Jiaotong University, Xi'an, Shaanxi 710049, China*
[b] *Reactor Science and Engineering Research Sub-institute, Nuclear Power Institute of China, Chengdu, Sichuan 610041, China*
[*] *Corresponding author: yqzheng@mail.xjtu.edu.cn*

[*]***Keywords:*** Unmanned Underwater Vehicles, Radiation Cavity, Heat Pipe Reactor

1. Introduction

Nuclear powered unmanned underwater vehicles (UUV), due to their advanced conceptual advantages and fearless performance in harsh environments, is one of the future directions for the development of unmanned underwater vehicles. Due to the wide range of engineering applications and mature technology of pressurized water reactors, the majority of ships with nuclear power systems are currently pressurized water reactors. But its drawbacks are obvious, such as complex equipment pipelines and difficulty in miniaturization. Besides, liquid cooled reactors rely on human control, making it difficult to achieve unmanned operation. Since its application in space nuclear reactor power supply in the 1960s, heat pipe reactors have experienced a period of decline, but in the early 21st century, due to the redesign of the US space exploration program, they have returned to the fore. And the success of heat pipe reactors such as Kilopower [1] in space reactor applications is evident, demonstrating the advantages and feasibility of heat pipe reactors in unmanned design.

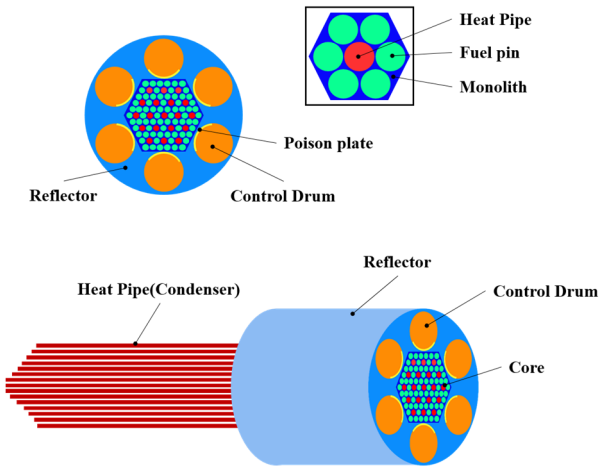

Fig 1 Schematic diagram of heat pipe reactor.

Heat pipe reactor refers to a solid-state reactor that uses heat pipes to passively export the heat from the core. It differs greatly from traditional reactors in terms of cooling methods and structural arrangements. It not only omits complex devices such as pipelines and pumps, but also simplifies the system structure and reduces costs. Due to the excellent performance of heat pipe reactors, research and development based on them are also ongoing, such as Heatpipe-operated Mars Exploration Reactor (HOMER) [2], the Heat Pipe Segmented Thermoelectric Module Converters Space reactor power system (HP-STMCs) [3], Martian Surface Reactor (MSR) [4], a kilowatt level power program developed by the United States (Kilopower), and a micro reactor developed by Westinghouse Electric Company (eVinci) [5], etc.

Different from the traditional reactors used on land, the unmanned reactor for underwater application has special requirements for radiation shielding. The concept of shadow shielding was adopted. Therefore, it only needs to provide shielding at the end to protect electrical equipment from radiation and ensure safe operation of the equipment and safe navigation. The design limits require that the cumulative neutron flux of the safety plane during full power operation be less than 10^{12} n·cm^{-2} and the cumulative photon dose be less than 10^{6} rad. However, if the heat pipe reactor applied for the unmanned underwater use, there will be a significant difference. To ensure the sufficient cooling of active core, there are a lot of heat pipes penetrating the end shield of the core and cause significant radiation cavity out of the traditional shielding area. Besides, in the water environment where the reactor works, the scattering of water will also cause radiation sources back to the system, which should be considered more to support the shielding design.

This paper investigated the radiation field of a heat pipe reactor design named UPRs [6] to show the impact of radiation cavity from the heat pipe penetration and the scattering of water out of the system.

Section 2 introduces the core configuration and current end shielding design of UPR-s. Section 3 analyzes the distribution of cumulative neutron flux and photon dose when the radiation cavity is considered. Section 4 discusses the influence of the scattering of seawater. Finally, Section 5 gives concluding remarks

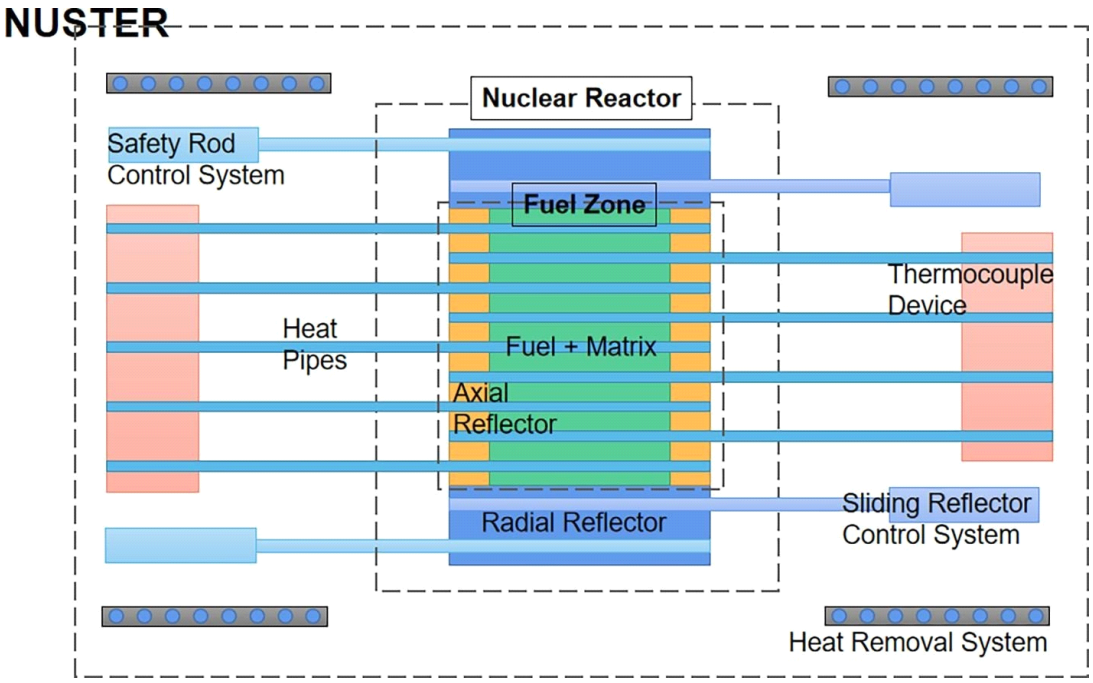

Fig 2 Brief schematics of NUSTER. [6]

2. Overview of UPR-s

2.1 Core configuration of UPR-s

UPR-s are applied to the power requirement of a NUclear Silence ThermoElectric Reactor system NUSTER [7], which is a multi-purpose nuclear power UUV, in the form of long water droplets. The concept design of NUSTER for the silent nuclear power system adopts the technical route of heat pipe cooling and thermoelectric conversion, and its silent characteristics can meet the needs of quiet operation.

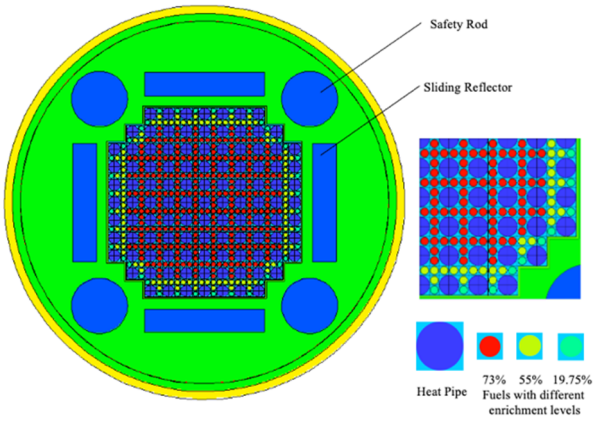

Fig 3 Core arrangement of UPR-s.

UPR-s is mainly designed for the needs of NUSTER. The core consists of a zone of fuel, insulation layer, fixed reflection layer, sliding reflection layer, safety rods, emergency exhaust channels, etc. Sodium heat pipes are used for cooling. An insulation layer is set outside the fuel zone, and a beryllium reflection layer is arranged outside the insulation layer. Boron carbide is used to surround the core to reduce mutual influence between the core and the external environment.

2.2 Current shielding design of UPR-s

For the shielding design, a circular composite cone shielding is used in UPR-s, with polyethylene placed on the inner side of the front end to shield neutrons, and tungsten on the outer side mainly used to reduce photon dose levels. Setting the shielding layer as a cone for the location of the source ensures both shielding effectiveness and quality reduction. In order to prevent the melting of polyethylene due to overheating, the water channels have been set up for cooling, and the stainless steel sleeves around the water channels are also conducive to reducing neutron flux and photon dose levels. And a tungsten layer was placed at the end of the shielding section to prevent secondary photons from being generated by the (n, γ) reaction of neutrons with the shielding material.

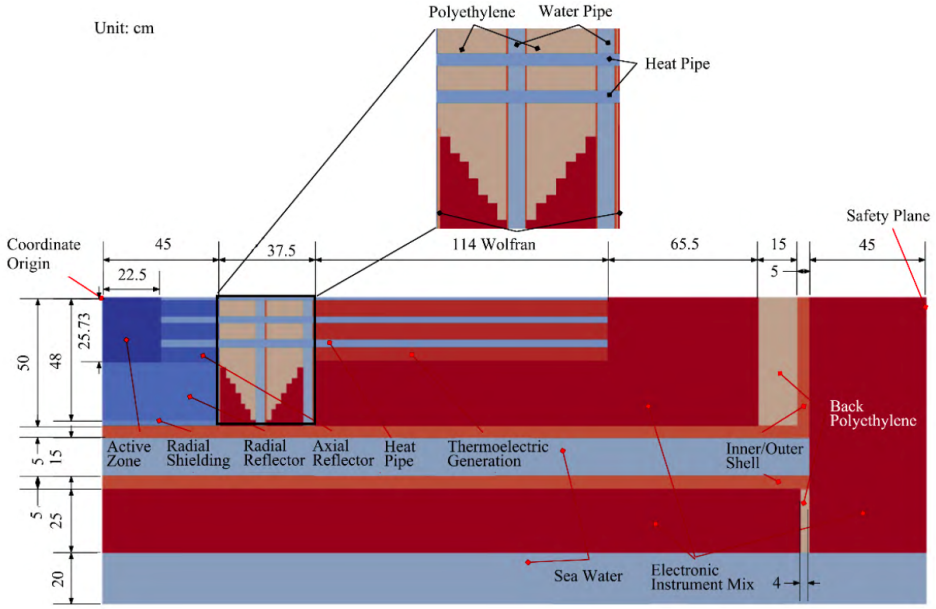

Fig 4 Shielding design of UPR-s. [8]

The shielding effect of this shielding design is shown in Table I, with a maximum neutron injection of $9.48*10^{11}$ and a maximum photon dose of $7.29*10^{5}$ as shown in Table I.

Table I: Shielding effect of UPR-s.

	safe plane (full power)	
	Cumulative neutron flux /n·cm^{-2}	Cumulative photon dose /rad
Design requirement	$\leq 10^{12}$	$\leq 10^{6}$
Final scheme	$\leq 9.48*10^{11}$	$\leq 7.29*10^{5}$

2.3 Comparison of different modeling methods

In this paper, the NECP-Hydra [9] program was adopted in the calculations. The program is a massive parallel S_N transport calculation program developed by the Nuclear Engineering Computational Physics (NECP) laboratory of Xi'an Jiaotong University. It is a three-dimensional code for radiation transport analysis based on S_N differential theory and utilizes advanced KBA parallel algorithms to achieve high parallel performance, supporting both rectangular and cylindrical geometry. [10]

Due to the fact that the structure of the heat pipe consists of four parts, including a sodium vapor chamber, a suction core, a sodium reflux gap, and a pipe wall, there are two options for modeling: detailed modeling and mixed modeling. In order to reduce the computational complexity while ensuring calculation accuracy, the two models were calculated and analyzed under the same calculation conditions. The modeling image is shown in Fig 5.

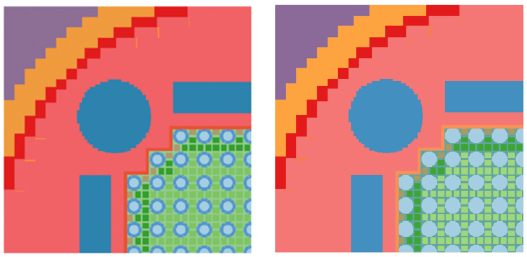

(a) Detailed modeling (b) Mixed modeling

Fig 5 Models with different modeling approaches.

The neutron flux and photon dose are compared along the axial distribution, the maximum difference calculated is 6.5% (neutron flux) and 1.7% (photon dose). The difference between the two modeling methods is within shielding limit (20%). Therefore, based on the calculation results, choosing mixed modeling can save computational resources and time while ensuring accuracy.

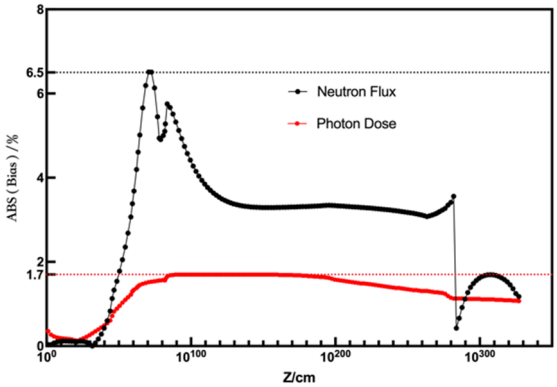

Fig 6 Bias of different modeling approaches.

According to the design of UPR-s, concrete modeling was conducted using NECP-Hydra, as shown

in the Fig 7.

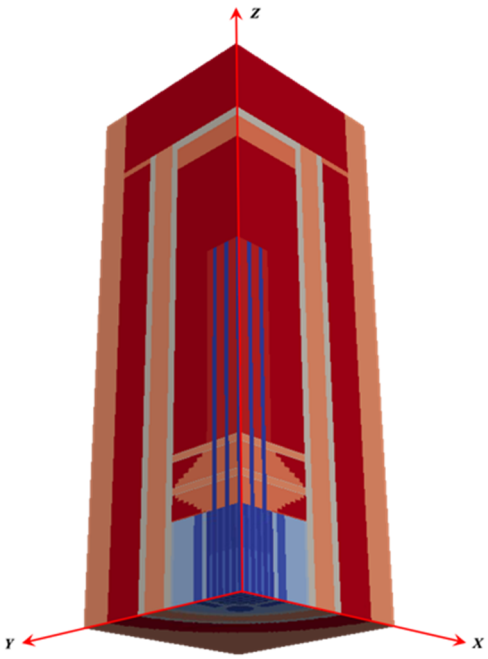

Fig 7 Model of Hydra.

3. Radiation cavity effects generated by heat pipes

3.1 Calculation of radiation distribution

Using NECP-Hydra for shielding calculation of this model, the neutron flux distribution can be obtained, shown as Fig 8. From the distribution, it can be seen that although the neutron flux at the safety plane is low, the key position of the unmanned underwater vehicle, which is the area where the control drive mechanism is located, has strong radiation and high flux levels.

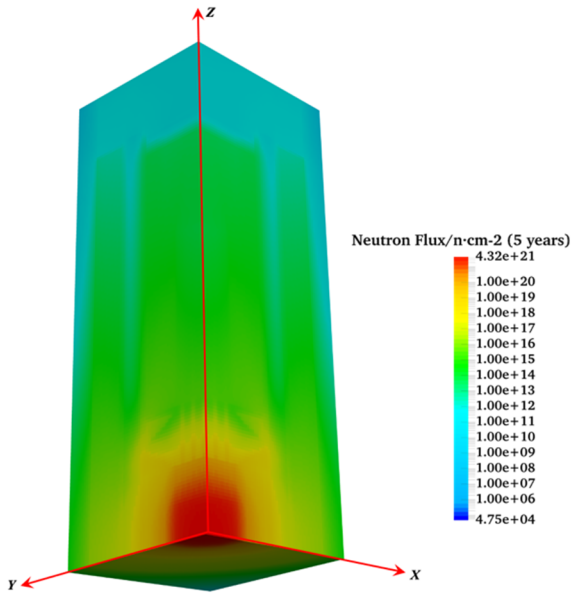

Fig 8 Neutron flux distribution.

According to the photon dose distribution in Fig 9, a preliminary conclusion can be drawn that as the axial height continues to increase, the photon dose tends to decrease, but still remains at a relatively high dose level (greater than 10^6). Due to the fact that current calculation and post-processing results can only be roughly judged, further exploration and calculation are needed.

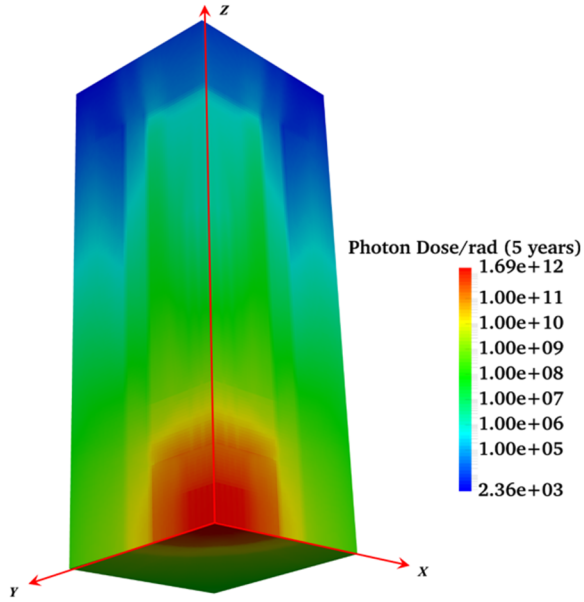

Fig 9 Photon dose distribution.

3.2 Calculation of the axial variation trend of radiation

In order to investigate the radiation distribution in the area of concern, several key locations were selected for analysis, namely in the core (0cm), in front of the shielding layer (45cm), behind the shielding layer (82.5cm), and at the back end of heat pipe (196.5 cm), as shown in Fig 10.

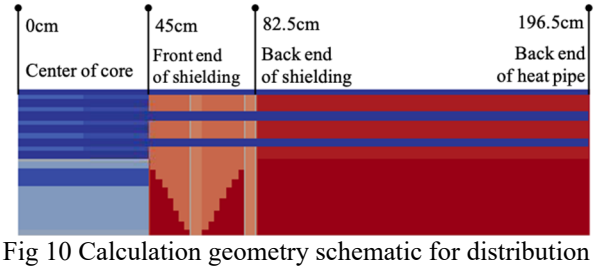

Fig 10 Calculation geometry schematic for distribution calculation.

From the distribution illustrated in Fig 11, it can be seen that the neutron radiation cavity generated by the heat pipe is distributed outward, and the areas with high neutron distribution gradually move outward along the axis.

As the axial height increasing, the area with high neutron flux continuously moves to the outer side of heat

pipe, where the electronic instrument is located and deposits.

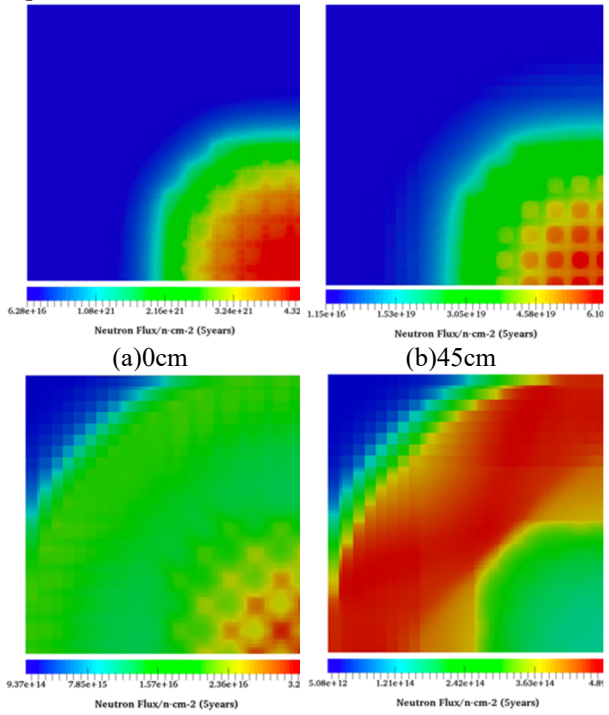

(a)0cm (b)45cm

(c)82.5cm (d)196.5cm

Fig 11 Distribution trend of Neutron Flux.

The distribution of photon dose is generally similar to that of neutron flux in terms of overall trend, showing a trend of moving towards the outer side of heat pipe. But the boundaries between high and low photon dose are clear, making it less likely to deposit in surrounding materials compared to neutrons. The distribution at the back of heat pipe (Fig 12(d)) also confirms this.

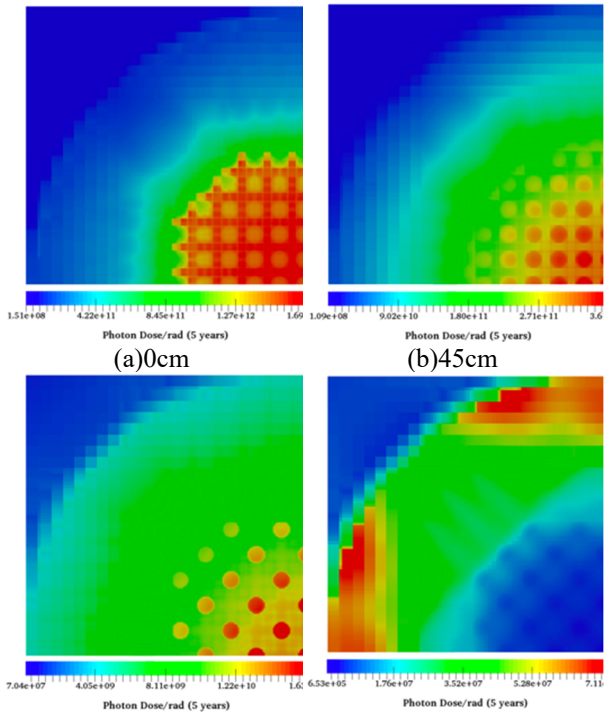

(a)0cm (b)45cm

(c)82.5cm (d)196.5cm

Fig 12 Distribution trend of Photon Dose.

3.3 Equipotential lines calculation

According to the trend of distribution of neutron flux and photon dose, this may mean that the radiation generated by the heat pipe reactor may be partially exported towards the outer end of heat pipe. Previously, the radiation from the heat pipe was considered to have been exported from the back end of the heat pipe, causing electronic instruments, operators, or maintenance personnel behind the heat pipe to receive excessive radiation, thereby increasing unnecessary risk.

But the new detailed results suggest that the electronic instruments at the outer end of heat pipe reactors are more likely to be affected. Taking the core profile (Fig 13) as an example to draw the neutron flux and photon dose equipotential lines here (Fig 14 and Fig 15)

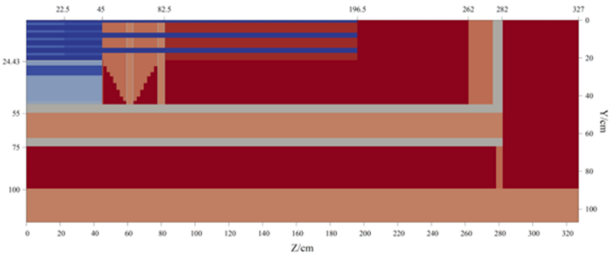

Fig 13 Computational geometry.

From the photon dose equipotential lines, it can be seen that although the overall value is small at the rear of the cavity, the dose limit of 10^6 in the core and shielding rear area (within the 55 cm range) does not begin to decrease until 190 cm, and the photon dose on the electronic instrument side even shows an upward trend.

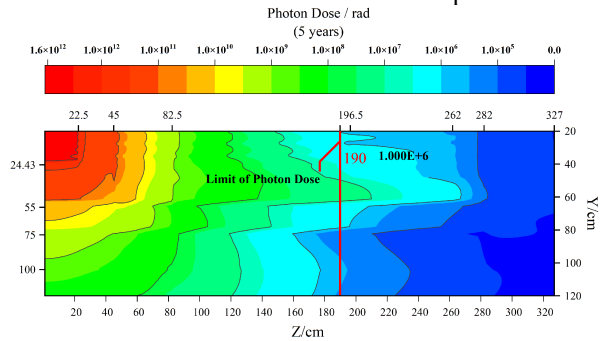

Fig 14 Equipotential lines of Photon Dose.

And the neutron flux value has always been in a relatively large magnitude, exceeding the limit value until 269 cm, which means that various instruments in the reactor have been in a radiation state exceeding the limit value.

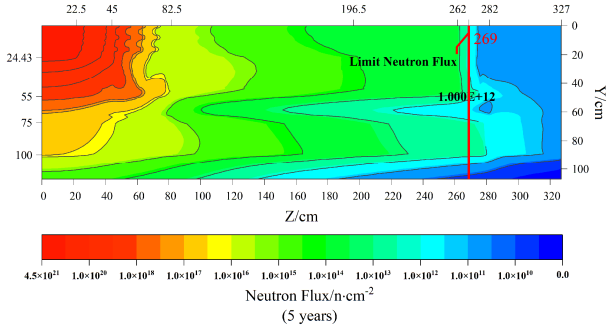

Fig 15 Equipotential lines of Neutron Flux.

From the analysis, it can be seen that the radiation in the key area where the electronic instrument is located exceeds the set limit, which is in an unsafe situation. This may lead to a reduction of the electronic instrument's life. Due to the fact that the instruments here may also include the driving mechanism of the control rods in the reactor, this problem may lead to serious consequences.

4. Scattering influence of seawater

For the application in the underwater environment, the scattering of seawater cannot be ignored. It may also cause an increase in neutron and photon flux, increasing the possibility of electronic instruments being exposed to radiation. In order to investigate the impact of seawater scattering, the area before seawater was selected for separate calculations and compared with the situation containing seawater.

In order to highlight the distribution trend of seawater influence, a partial shielding is added around the shielding and heat pipes to reduce the radiation cavity here. Calculation and analysis are conducted using it (with density of 1 g/cm^3). Since 50 cm is the main area, the areas within this section were selected for comparison, as shown in Fig 16. For photon dose, the difference is not significant in two different situations. The limit value of 10^6 is basically reached at an axial position of 174 cm.

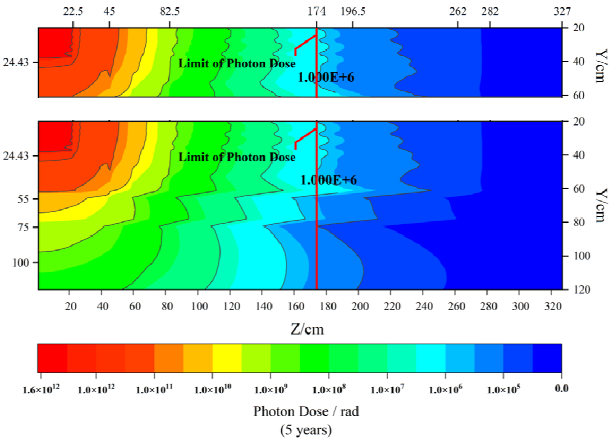

Fig 16 Comparison of photon dose for the two cases.

The difference in neutron flux levels is significant, and it is clear from the Fig 17 that the entire equipotential line is moving towards the back due to seawater. In the area at the back of the electronic instrument, the limit value of 10^{12} has a maximum height of 141 cm without the influence of seawater. Due to the influence of seawater, this limit has moved to a position of 154 cm.

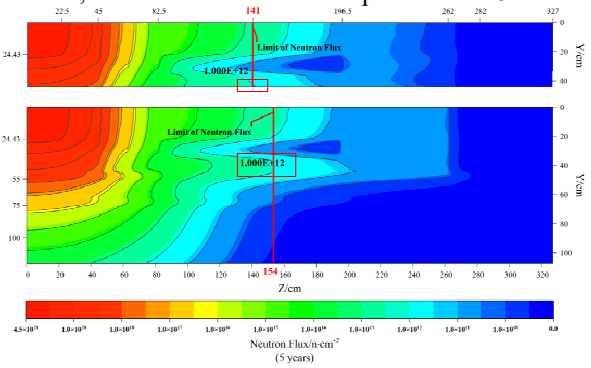

Fig 17 Comparison of neutron flux for the two cases.

The calculation area within 50 cm in both cases was calculated according to axial stratification, and the calculated photon dose increased due to the influence of seawater were displayed on Fig 18.

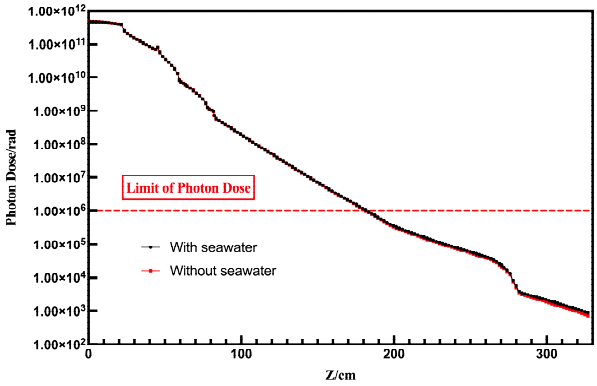

Fig 18 Changes along the axial direction in two situations.

Similar to the results shown in the equipotential distribution, the influence of seawater on photons is relatively small, and the distribution of the two curves is not significantly different. The axial distribution of the increment of neutron flux due to the influence of seawater is shown in Fig 19

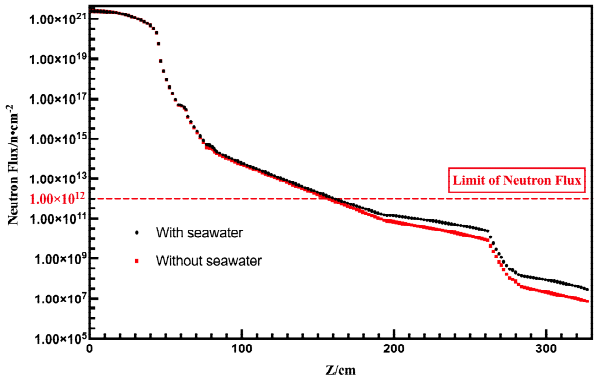

Fig 19 Changes along the axial direction in two

situations.

The influence of neutron distribution caused by seawater is greater than that of photon. Throughout the axial direction, due to the influence of seawater, the curve is at a higher position, especially below the design limit.

It is found that although the radiation level of the safety plane calculated in the end is lower than the standard limit, the key areas during the shielding process are not effectively protected, resulting in the radiation they bear exceeding the limit, which can easily lead to radiation risk.

5. Conclusion and Summary

The main work of the paper is to investigate the radiation field of the UPR-s heat pipe reactor in a nuclear powered UUV. The values and distribution of neutron flux and photon dose after five years of full power operation were calculated. It is found that the radiation transports outward along the axis of heat pipes, causing the neutron flux and photon dose surrounding the heat pipes much higher than expected. Therefore, the surrounding area is not suitable for arranging electronic instruments without additional local shield.

In addition, due to the impact of underwater environment, the consideration of seawater's scattering is necessary. There are significant changes in neutron flux and photon dose levels in key areas with and without considering the scattering effects. Ignoring this effect leading to an increase in radiation to electronic instruments and an increase in the likelihood of instrument damage leading to other conditions.

In summary, this paper analyzed the radiation field and investigated the differences in the shielding requirement of underwater heat pipe reactors. It will be the reference for the shielding design of this heat pipe reactor in the future.

REFERENCES

[1] Gibson M A, Mason L, Bowman C, et al. Kilopower, NASA's small fission power system for science and human exploration[C]//12th International Energy Conversion Engineering Conference. USA, 2014. DOI: 10. 2514/6.2014-3458

[2] Poston D I. The heatpipe-operated mars exploration reactor (HOMER) [C]//AIP Conference Proceedings. Albuquerque, New Mexico. AIP, 2001. DOI: 10.1063/1.1358010.

[3] El-Genk M S. Conceptual design of HP-STMCs space reactor power system for 110 kWe[C]//AIP Conference Proceedings. Albuquerque, New Mexico (USA). AIP, 2004. DOI: 10.1063/1.1649628.

[4] Bushman A, Carpenter D M, Ellis T S, et al. The martian surface reactor: an advanced nuclear power station for manned extraterrestrial exploration, MIT-NSA-TR-003 [R]. Massachusetts Institute of Technology, 2004.

[5] Levinsky A, van Wyk J J, Arafat Y, et al. Westinghouse eVinci reactor for off-grid markets[C]. Transactions of the American Nuclear Society, USA, 2018.

[6] Du X N, Tao Y S, Zheng Y Q, et al. Reactor core design of UPR-s: a nuclear reactor for silence thermoelectric system NUSTER[J]. Nuclear Engineering and Design, 2021, 383: 111404. DOI: 10.1016/j. nucengdes. 2021. 111404.

[7] Tang, S., Wang, C., Zhang, D., Tian, W., Su, G., Qiu, S., 2021. Thermoelectric performance study on a heat pipe thermoelectric generator for micro nuclear reactor application. Int. J. Energy Res. 45 (8), 12301–12316.

[8] Wang Y, Tao Y, Wu Y, Zheng Y, Design study of shielding scheme for megawatt-scale heat pipe nuclear reactors [J]. Nuclear technology,2023,46(02):113-126.(In Chinese)

[9] Xu, L., Cao, L., Zheng, Y., et al., 2017. Development of a new parallel SN code for neutronphoton transport calculation in 3-D cylindrical. Prog. Nucl. Energy 94 (1), 1–21.

[10] Wang Y, Zheng Y, Xu L, et al. NECP-hydra: A high-performance parallel S code for core-analysis and shielding calculation[J]. Nuclear Engineering and Design, 2020,366: 110711.